PAPER

Check for updates

Selective and sustainable nitro reduction and reductive *N*-alkylation using a recyclable V$_2$O$_5$/TiO$_2$ catalyst for amine synthesis

Rahul Upadhyay,[ab] Shashi Kumar,[ab] Kancharlapalli Srinuvasu,[cd] Chinnakonda S. Gopinath, [ID][e] K. R. S. Chandrakumar [ID] *[cd] and Sushil K. Maurya [ID] †*[ab]

We present a sustainable and versatile catalytic platform for the synthesis of primary and secondary amines *via* the selective reduction of nitroarenes, employing a heterogeneous V$_2$O$_5$/TiO$_2$ catalyst. This methodology eliminates the use of stoichiometric metal hydrides, molecular hydrogen, and homogeneous catalytic systems, aligning with green chemistry principles. The catalyst exhibits excellent chemoselectivity across a diverse array of nitroarenes, including substrates bearing alkenes, alkynes, halogens, and functionalized heterocycles, demonstrating broad functional group tolerance. Furthermore, we extend this platform to a one-pot reductive alkylation of nitroarenes with alkyl halides (Br and I), affording *N*-alkylated amines in high yields under mild conditions. The catalytic system is recyclable over multiple cycles with minimal loss of activity or selectivity, showcasing its practical utility. The synthetic value of this approach is highlighted through the preparation of 47 (hetero)arylamines, 12 secondary amines, and 7 pharmaceutically relevant molecules, including paracetamol, phenacetin, and bromhexine. Mechanistic insights derived from DFT calculations and controlled experiments provide a molecular-level understanding of the selective nitro group activation on the V$_2$O$_5$/TiO$_2$ surface. This work contributes a green, efficient, and mechanistically informed catalytic solution for amine synthesis from abundant nitroarenes.

[a] *Chemical Technology Division, CSIR-Institute of Himalayan Bioresource Technology Palampur, Himachal Pradesh, 176 061, India. E-mail: sushilncl@gmail.com*

[b] *Academy of Scientific and Innovative Research (AcSIR), Ghaziabad, 201 002, India*

[c] *Theoretical Chemistry Section, Bhabha Atomic Research Centre, Mumbai 400 085, India. E-mail: krsc@barc.gov.in*

[d] *Homi Bhabha National Institute, Mumbai 400 094, India*

[e] *Department of Chemistry, Indian Institute of Technology Palakkad, Kanjikode, Palakkad 678 623, India*

† Present address: Department of Chemistry, Faculty of Science, University of Lucknow, Lucknow, Uttar Pradesh, 226 007, India

Introduction

Owing to the broad applicability of amines in the preparation of pharmaceuticals, agrochemicals, polymers, and dyes, the development of efficient processes for their synthesis is an area of intense research.[1–4] Nitro compounds are widely used to synthesize industrially important precursors such as amines,[5–8] azides,[9] hydroxyl amines,[10,11] and azo compounds.[12,13] The catalytic reduction of nitroarenes represents a most benign and classical method for preparing a diverse range of functionalized amines in chemical industries. In the past decades, the industry utilized RANEY® nickel and hydrogen gas to reduce nitroarenes, which are associated with several hazards like an explosion. Various noble metal-catalysed processes using Pd, Au, Ag, and Rh-based catalysts were reported to reduce nitro compounds to their respective amines.[14–20] Apart from this, other metal-based catalytic systems were also used, which include Sn, V, Cr, Fe, Co, Ni, and Zn, but these catalytic systems require stoichiometric amounts of acids/bases for treatment, a long reaction time, *etc.* for the reduction of nitro compounds.[1,21–28] The previously reported methods utilized toxic and expensive metal catalysts, cumbersome catalyst synthesis, hazardous reaction conditions, and stoichiometric amounts of reducing agents. In the case of a homogenous catalytic system, the products are often contaminated with metals. Their removal adds an extra step and raises environmental and complicated alarming health hazards, which demand the safe disposal of these metals and by-products.[29,30] The previous methods also suffer from competitive halogenation/dehalogenation, alkene/alkyne reduction, a prolonged reaction time, and generation of by-products, which lead to the reduction in atom economy of the process (Fig. 1B). Recently a few groups have reported catalytic systems for the reduction of nitroarenes utilizing hydrazine hydrate in stoichiometric amounts.[31,32]
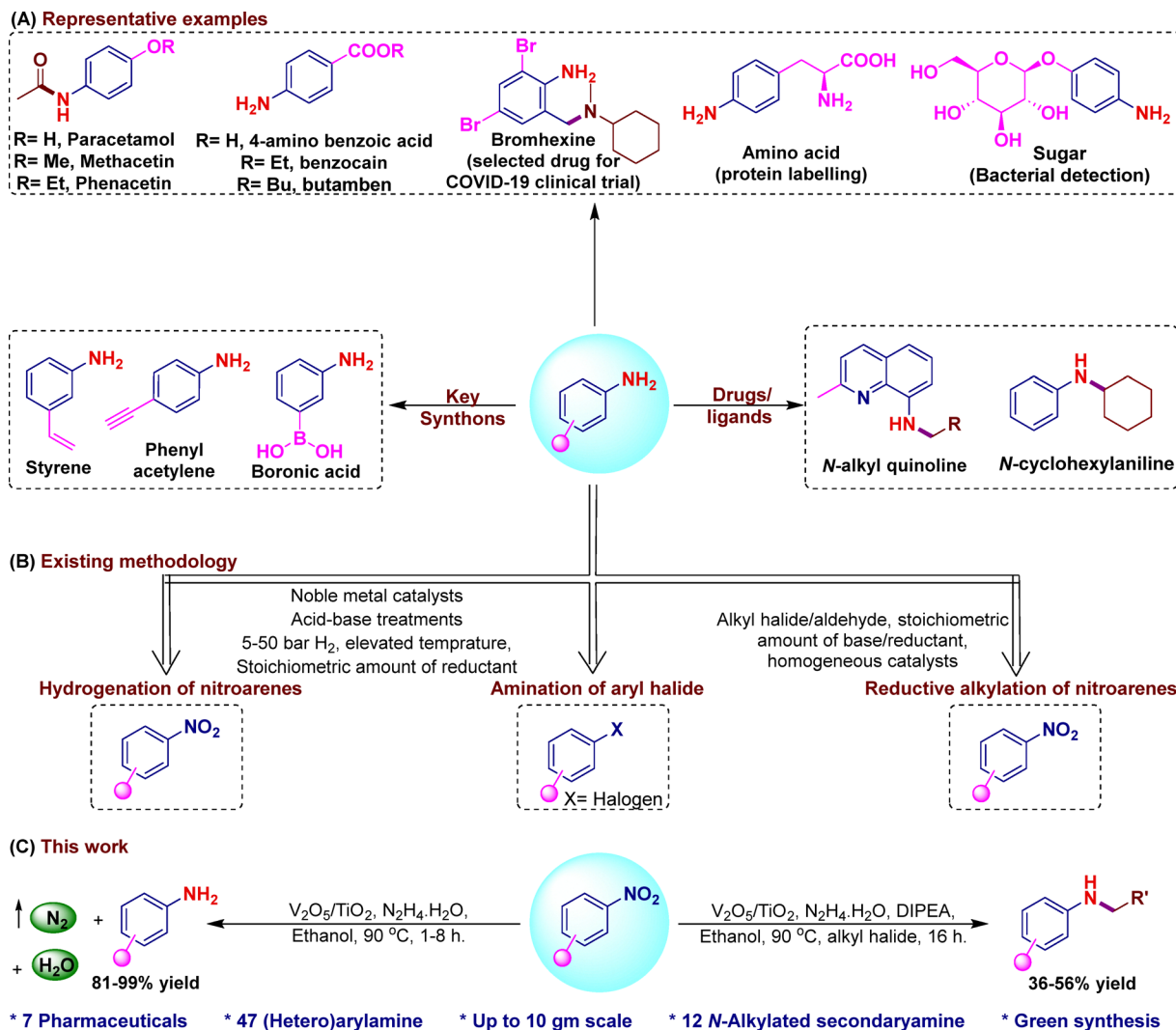
Fig. 1 (A) Representative examples, (B) existing methodology for the synthesis, and (C) waste-free reduction and N-alkylation of nitroarenes (this work).

To overcome these challenges, here we report a recyclable heterogeneous V_2O_5/TiO_2 catalysed efficient methodology for the reduction of nitro compounds to their respective amines in good to excellent yields (Fig. 1C). The developed protocol requires low catalyst loading, green solvents, moderate temperature, and a smaller amount of reducing agent. Recently in 2021, we reported the utilization of vanadium catalysts for the sustainable synthesis of carboxylic acid from olefins.[33] Furthermore, for this study, we have synthesized the V_2O_5/TiO_2 catalyst system with various strengths using a modified procedure.[33] Due to the vast application of alkylated amines, the direct alkylation of nitroarenes for the synthesis of secondary and tertiary amines has gained much attention in recent times. In the past decades, these amines were mainly synthesized by utilizing Buchwald–Hartwig coupling,[34] Ullmann coupling,[35] aminations of carbonyls and alcohols,[36,37] and alkylation of anilines with alkyl halides.[38] Among these, the direct alkylation reaction utilizes a stoichiometric amount of a base. These amines are usually prepared by reducing nitroarenes, which adds an extra step to the alkylation. Recently a few

methodologies have been reported to synthesize N-alkylamines via direct reductive alkylation of nitroarenes.[39–41]

Results and discussion

Catalyst preparation and characterization

The catalysts V_2O_5/TiO_2 were prepared via the sol–gel method utilizing vanadium pentoxide and titanium(IV) butoxide. TiO_2 was selected as the support due to the compatibility of the Ti^{4+} ionic radius and oxidation state with those of vanadium, which facilitates strong metal–support interactions and improved catalyst stability. Unlike non-redox supports such as SiO_2 and Al_2O_3, TiO_2 can participate in redox processes, which may enhance the catalytic performance. These factors make TiO_2 a more suitable support material for this study. Using the method, we synthesized V_2O_5 supported over TiO_2 with various strengths (C-05, C-10, and C-20) and characterized them using different techniques.[33] Moreover, in continuation here we

perform X-ray photoelectron spectroscopy (XPS) to provide detailed information about the catalysts. The V 2p core level spectrum was recorded for three different catalysts containing 10%, 20%, and 30% V_2O_5. The intensities of the V 2p spin–orbit core levels for all catalysts were normalized to the 20% V_2O_5 sample to facilitate direct comparison of binding energy (BE) changes and the full-width at half-maximum (FWHM) of the core-level features. The 20% V_2O_5-loaded catalyst exhibited the largest FWHM of 2.7 eV with a peak maximum at a BE of 517.2 eV, while the 30% V_2O_5 catalyst showed the smallest FWHM of 2.0 eV at a lower BE of 516.7 eV. This significant decrease in FWHM and the lower BE for the 30% V_2O_5 catalyst suggest that vanadium is predominantly in the 4+ oxidation state. In contrast, both V^{4+} and V^{5+} oxidation states are evident in the 10% and 20% V_2O_5 catalysts, as indicated by the higher BE and broader spectral features. The intensity-normalized V 2p core-level features further confirm broadening on the higher BE side in the 10%, 20%, and 30% V_2O_5 catalysts, while the lower BE side remains consistent across all compositions. However, the broadening observed at the onset of the V $2p_{3/2}$ feature for the 20% V_2O_5 catalyst suggests a relatively high or at least comparable amount of V^{4+} to the other catalysts. This highlights the presence of a unique combination of V^{4+} and V^{5+} oxidation states in the 20% V_2O_5 catalyst, which correlates with its superior catalytic performance (Fig. 2(A)). A representative V $2p_{3/2}$ core level result is shown in the inset of Fig. 2A for the best performing 20% V_2O_5/TiO$_2$ catalyst. A very similar result observed, to that of a fresh catalyst, directly demonstrates the robustness of the catalyst to withstand the reaction conditions. Although the redox couple of V^{4+}/V^{5+} could undergo changes under reaction conditions, very similar results observed before and after reaction underscore the preservation of mixed valence states at the end of the reaction. Indeed, several cycles of reactions carried out testify this conclusion of preservation of mixed valence states, irrespective of the reaction conditions.

The Ti 2p core levels were also analyzed by XPS, and the results, shown in Fig. 2(B), were obtained after deconvolution. All three catalysts exhibit a Ti^{3+} component at 457.3 ± 0.1 eV, accounting for 3–6% of the total Ti, while Ti^{4+}, observed at 458.5 ± 0.1 eV, is the predominant oxidation state. This indicates that the primary role of TiO$_2$ is as a support material. Ti 2p spectral features of the spent catalyst remain the same as those of the fresh catalyst, reiterating the maintenance of mixed valence states, irrespective of the reaction conditions. Previously, we have explored the oxidation potential of these synthesized catalysts over various scaffolds.[42–44] Building upon this research, we now shift our focus towards exploring their potential in reduction reactions. Specifically, we are interested in utilizing these catalysts for the reduction of nitroarenes into their corresponding amines.

Catalyst screening and optimization of the reaction conditions

To begin our investigation, nitrobenzene was selected as a model substrate to optimize the reaction conditions. Initially, nitrobenzene (0.5 mmol) was dissolved in ethanol (2 mL) and V_2O_5/TiO$_2$ catalyst (10 wt%) of different strengths (C-05, C-10, and C-20) and hydrazine hydrate (25 equiv.) were added to it, and the resulting reaction mixture was then stirred at 25 °C up to 12 hours, but a trace of the product was observed with the C-20 catalyst (Table S1, entries 1–3). However, no reaction was observed when the reaction was performed in other solvents (Table S1, entries 4–7). Next, the reaction temperature was optimized using ethanol as a solvent, and to our delight, an excellent yield of the desired amine was obtained at 90 °C in 1.0 h (Table S1, entries 8–10). However, lowering the catalyst strength to 10% at 90 °C resulted in a decrease in the product yield (Table S1, entry 11). Reducing agents other than hydrazine hydrate resulted in no reaction under similar conditions (Table S1, entries 12–14). Furthermore, the amount of reducing agent was optimized, and three equivalents of hydrazine
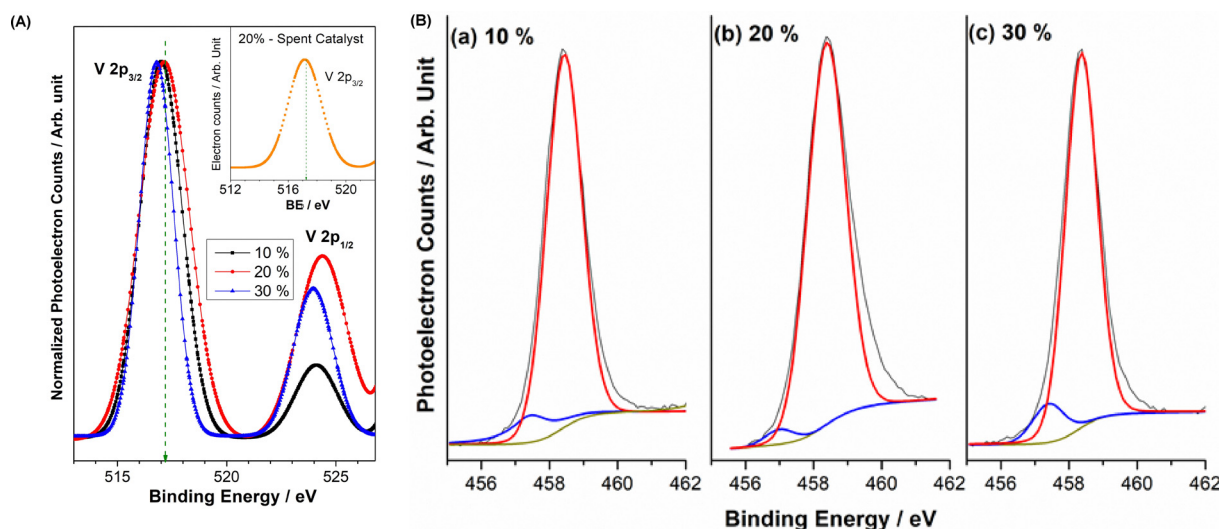

Fig. 2 (A) Vanadium 2p core level spectra recorded for different loadings of V_2O_5 supported on TiO$_2$ and the spent catalyst. (B) Titanium 2p core level spectra recorded for different loadings of V_2O_5 supported on TiO$_2$.
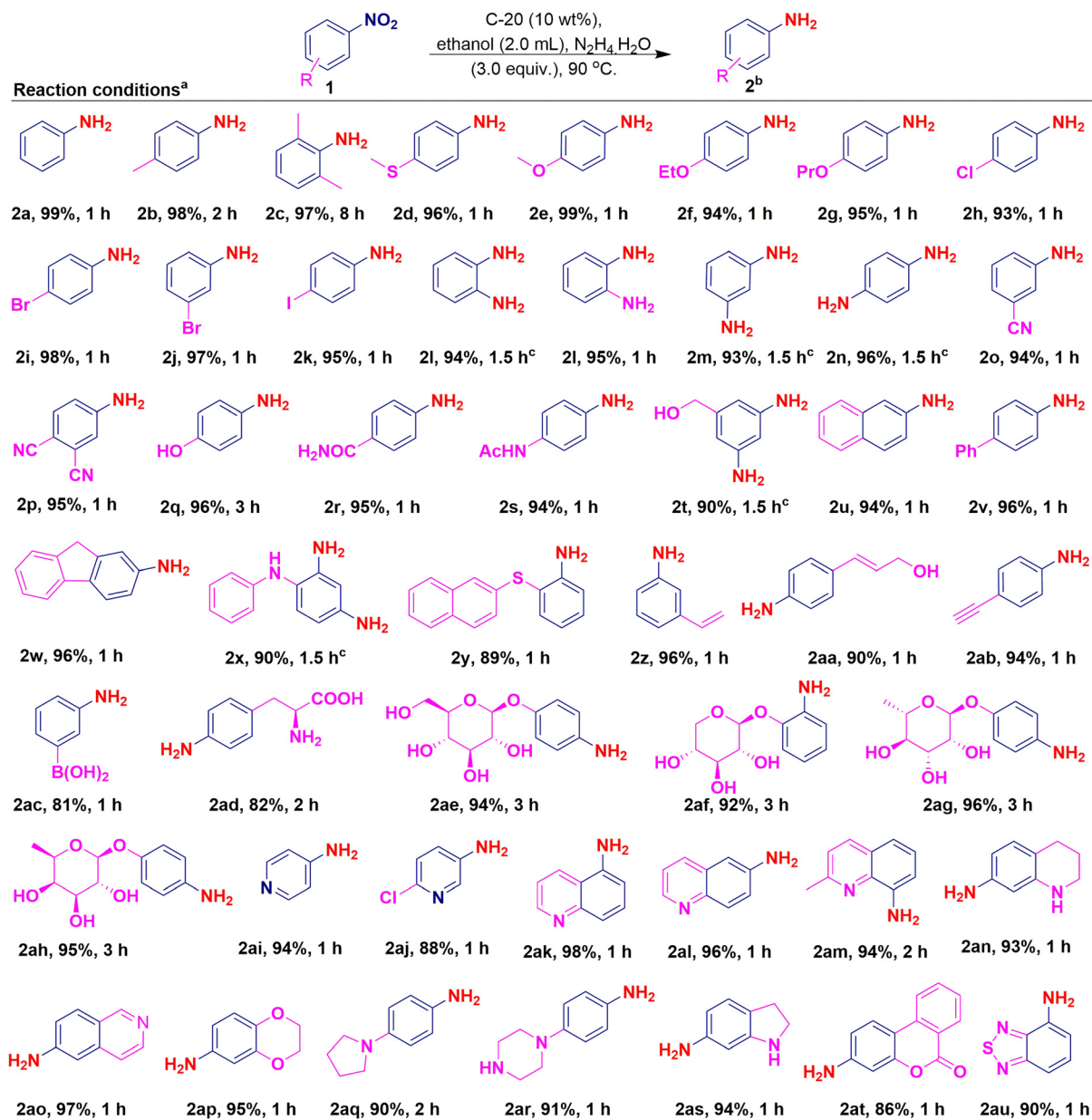
hydrate were found to be sufficient for the complete conversion (Table S1, entries 15–18). The amount of catalyst loading directly affects the yield, and a significant decrease in the yield of the product was observed when the amount of the catalyst was reduced from 10 to 7.0 wt%. (Table S1, entry 19). No reaction was observed in the absence of either a reducing agent or a catalyst (Table S1, entries 20 and 21). Surprisingly, the reaction does not occur when parent TiO_2 and V_2O_5 were used separately to catalyse the reaction (Table S1, entries 22 and 23).

Substrate scope for the reduction of nitroarenes

We began our endeavor to study substrate compatibility for the developed protocol with optimized conditions in hand

(Table S1, entry 18). Accordingly, the methyl-substituted nitroarenes were transformed into their corresponding anilines in excellent yields (Scheme 1, **2b** and **2c**). The methoxy and methylsulfane substituted nitroarenes provided the desired amine in excellent yields (Scheme 1, **2d** and **2e**). The ethoxy and propoxy derivatives were smoothly converted into their respective amines (Scheme 1, **2f** and **2g**). Halogenated amines are the key intermediates for the agrochemicals; however, halogen substituents on nitroarenes are susceptible to dehalogenation during reduction under hydrogenation conditions and are challenging substrates for this transformation.[45] Different halogenated substrates were subjected to the developed reaction conditions, and interestingly, a good yield of corresponding amines was obtained

Scheme 1 Substrate scope for the reduction of nitroarenes. [a] Reaction conditions: nitroarenes **1** (1.0 equiv., 100 mg), C-20 (10 wt%), $N_2H_4 \cdot H_2O$ (3.0 equiv.), ethanol (2.0 mL), 90 °C for 1–8 h, [b] isolated yield, and [c] $N_2H_4 \cdot H_2O$ (6.0 equiv.).
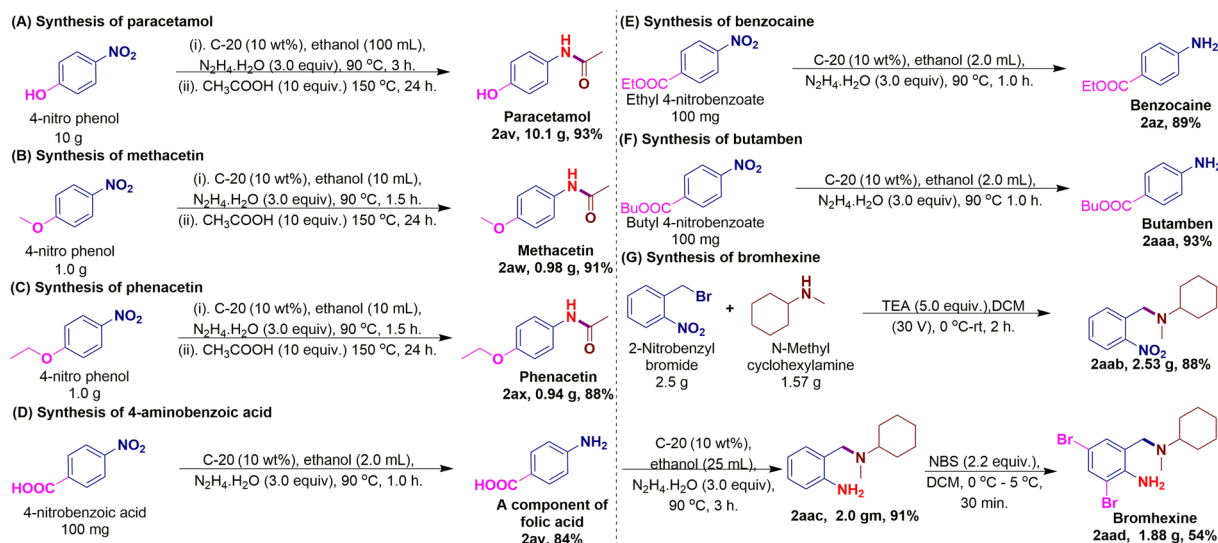
without affecting the substitution over the benzene ring (Scheme 1, **2h–2k**). The developed methodology was found to be efficient for reducing *ortho*, *meta*, and *para*-substituted dinitroarenes, and comparable yields of diamine products were obtained (Scheme 1, **2l–2n**). Nitrile-substituted nitroarenes were well tolerated and furnished the desired amines in excellent yields with excellent selectivity towards the nitro reduction (Scheme 1, **2o** and **2p**). The *p*-hydroxy nitrobenzene provided a quantitative yield of the desired aniline (Scheme 1, **2q**). Benzamide and acetanilide derivatives of nitrobenzene were effectively reduced to their corresponding aniline derivatives in good to excellent yields without the formation of any by-product (Scheme 1, **2r** and **2s**). Synthesis of 3,5-diamino benzyl alcohol was achieved by reducing 3,5-dinitrobenzyl alcohol, which is an important intermediate for the synthesis of 9-anilinothiazolo[5,4-*b*] quinoline derivatives as potential antitumoral and 4-anilinoquinoline derivatives as potential antimalarial agents (Scheme 1, **2t**).[46,47] The nitro derivatives of naphthalene, biphenyl, and fluorene were efficiently reduced to their respective amines in excellent yields (Scheme 1, **2u–2w**). The synthesis of 2,4-diaminodiphenylamine was successfully achieved in 90% yield utilizing respective dinitro derivatives (Scheme 1, **2x**). The naphthalen-2-yl(2-nitrophenyl)sulfane derivative was reduced efficiently to its corresponding 2-(naphthalen-2-ylthio)aniline ion with 89% yield (Scheme 1, **2y**). Furthermore, the hetero and unsaturated nitro compounds were tested for their feasibility towards reduction under developed protocols. It was observed that the method was efficient in reducing them to their corresponding amines. The selective reduction of challenging substrates, such as 3-nitro styrene, was achieved with excellent yield and selectivity; pleasingly, no double bond reduction was observed under developed reaction conditions (Scheme 1, **2z**).[48,49] The cinnamyl alcohol bearing nitro-group were tolerated well to furnish the corresponding amine in an excellent yield (Scheme 1, **2aa**). Similarly, an excellent yield was obtained when reducing nitro-substituted phenylacetylene derivatives, where the alkyne

was unaffected under developed reaction conditions (Scheme 1, **2ab**).[50] The nitroarene containing important functionalities such as boronic acid, which is frequently utilized for different chemical transformations, was subjected to the developed protocol, and pleasingly a good yield of the desired amine was obtained (Scheme 1, **2ac**).[51] Interestingly, the amino acid derivative 4-nitro-L-phenylalanine gave the corresponding 4-amino-L-phenylalanine in good yield, which is an important compound used in protein labelling (Scheme 1, **2ad**).[52] In the continuation, the sugar derivatives of nitroarenes transformed smoothly into their corresponding amines in good to excellent yields (Scheme 1, **2ae–2ah**). The heterocyclic nitro derivatives, such as 4-nitropyridine and 2-chloro-5-nitropyridine, resulted in good yields of their respective amines (Scheme 1, **2ai** and **2aj**). To our delight, medicinally important compounds, such as nitro-substituted quinoline derivatives, provided an excellent yield of aminoquinolines (Scheme 1, **2ak–2am**). The tetrahydroquinoline derivative was also transformed into its respective amine (Scheme 1, **2an**). Moreover, the isoquinoline derivative yielded the desired amine in excellent yield (Scheme 1, **2ao**). The nitro derivative of benzo dioxane reacted well under the developed reaction conditions and gave the desired amine in a 95% yield (Scheme 1, **2ap**). The optimal yield of the desired 4-(pyrrolidine-1-yl) aniline was obtained from the reduction of 1-(4-nitrophenyl) pyrrolidine (Scheme 1, **2aq**). 4-(Piperazin-1-yl)aniline was obtained in 91% yield from its respective nitro derivative (Scheme 1, **2ar**). Interestingly, the indoline and benzochromenone derivatives provided 94 and 86% yields, respectively (Scheme 1, **2as** and **2at**). The nitro derivative of benzothiadiazole was efficiently converted into its respective amine in good yield (Scheme 1, **2au**).

Synthetic application in medicinal chemistry

A one-pot transformation of 4-nitrophenol to a pharmaceutically active molecule, *i.e.*, paracetamol, in good yield at a 10 g

Scheme 2 Synthesis of the important pharmaceuticals: (A) paracetamol; (B) methacetin; (C) phenacetin; (D) 4-aminobenzoic acid; (E) benzocaine; (F) butamben; (G) bromhexine.

scale further demonstrated the versatility of the developed protocol (Scheme 2, **2av**). Paracetamol is a frequently used over-the-counter drug in clinical practice, including for patients suffering from COVID-19, and has been synthesized using different protocols, mostly in multiple steps.[38,53] By utilizing similar reaction conditions, other parallel pharmaceuticals, such as methacetin and phenacetin, were also synthesized in good yields (Scheme 2, **2aw** and **2ax**). The synthesis of 4-amino benzoic acid, which is a component of folic acid, was successfully achieved in good yield (Scheme 2, **2ay**). The synthesis of other medicinally important molecules, such as benzocaine and butamben, which are used as anesthetic drugs, was accomplished smoothly (Scheme 2, **2az** and **2aaa**). Bromhexine, another important active pharmaceutical ingredient, is a mucolytic drug used to treat respiratory tract infections associated with excess mucus.[54] The previous synthetic protocol for bromhexine utilized RANEY® nickel to reduce the nitro group to its respective amine. Herein, we used a recyclable heterogeneous catalytic system to reduce the nitro functionality into the corresponding amine in 91% yield (Scheme 2, **2aab**). The resulting compound was finally reacted with N-bromosuccinimide to obtain bromhexine in 54% yield (Scheme 2, **2aad**).
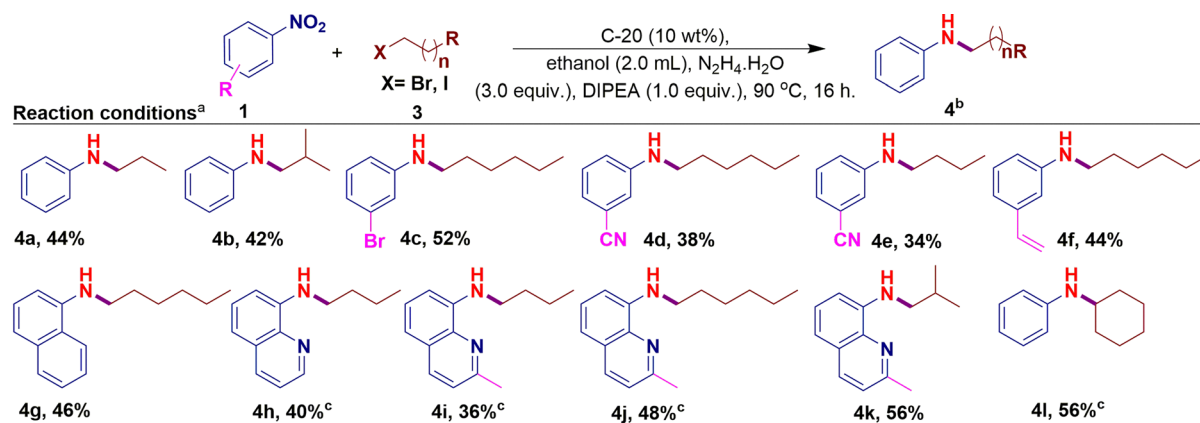
Reductive alkylation of nitroarenes

The reductive alkylation of the nitroarenes into their respective amines was successfully achieved (Scheme 3). Exclusively, the monoalkylated amines were formed, and a low selectivity towards the dialkylated amine was observed under the developed protocol. The nitrobenzene was alkylated with propyl and isobutyl halides in 44% and 42% yields, respectively, under developed reaction conditions (Scheme 3, **4a** and **4b**). The bromo-substituted nitrobenzene derivative was successfully transformed into its corresponding amine in good yield (Scheme 3, **4c**). The nitrile-substituted nitroarenes were found to be compatible and provided the desired product in 38 and 34% yields (Scheme 3, **4d** and **4e**). 3-Nitro styrene was alkylated under developed reaction conditions with a 44% yield (Scheme 3, **4f**). 1-Nitronaphthalene gave the corresponding amine in good yield (Scheme 3, **4g**). 8-Nitroquinoline and 8-nitroquinaldine selectively gave monoalkylated products utilizing 5.0 equiv. of alkyl halide (Scheme 3,

4h–4k). In the case of a secondary alkyl halide, the selectivity towards the monoalkylated product was relatively high as compared to a primary alkyl halide, and the cyclohexyl iodide provided the respective amine in good yield (Scheme 3, **4l**). When the reaction was performed using aromatic halides, *i.e.*, benzyl bromide, it resulted in no desired products, and the formation of hydrazine hydrobromide was observed. This is because of the quick release of bromide ions from benzyl bromide, which combine with their counter ions, *i.e.*, hydrogen ions, to form hydrogen bromide.

Catalyst recyclability and comparison studies

Catalyst stability and recyclability are the crucial performance metrics to assess a catalytic protocol's cost-effectiveness and translational potential. The recyclability of the catalyst was evaluated using nitrobenzene as a substrate under optimized reaction conditions. No considerable decrease in the yield of the desired amine up to six cycles was observed, and the catalyst was found to be efficient in performing the reduction after every reaction cycle without significant loss in the yield. The catalyst was recycled by centrifugation or filtration after each cycle, and the residual catalyst was washed with ethanol or acetone and dried in an oven for 2 h at 100 °C and reused (Fig. 3A). Further to access the synthetic viability and sustainability of the developed protocol for paracetamol synthesis over the reported one-pot synthetic methodology, a comparison with the existing methods was performed. The study found that most of the protocols utilize a noble metal (Pt[55,56] and Ru[57]), a Co–Mo–S catalyst using 11 bar H_2,[50] and controlled substances like acetic anhydride (Fig. 3B). Here in this case, we performed the reaction under greener conditions (green solvent, heterogeneous catalyst, and non-hazardous by-product formation), column-free, and at a multi-gram scale (0.1–10 g). To study the reaction's progress with time, typical ^{1}H NMR spectra of the crude reaction mixture were recorded at different time intervals, and all the obtained spectra were stacked on the same scale. The study resulted in the steady progress of the reaction at the beginning, concerning product formation. It was observed that the reactant concentration was consumed more

Scheme 3 Reductive alkylation of nitroarenes. [a] Reaction conditions: nitroarenes **1** (1.0 equiv., 50.0 mg), alkyl halide **3** (3.0 equiv.), C-20 (10 wt%), $N_2H_4\cdot$ H_2O (3.0 equiv.), DIPEA (1.0 equiv.), ethanol (2 mL), 90 °C for 16 h, [b] isolated yield, and [c] alkyl halide **3** (5.0 equiv.).
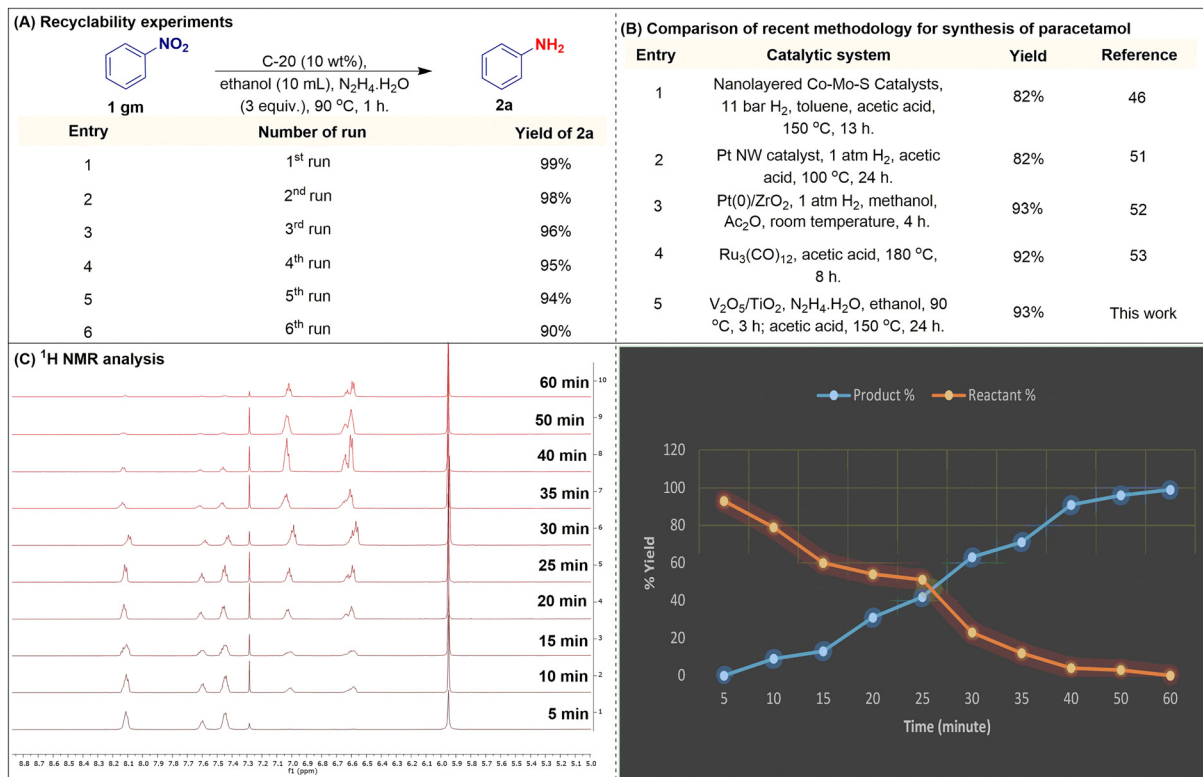
Fig. 3 (A) Recyclability experiment, (B) comparison studies and (C) ^{1}H NMR results of the crude reaction mixture at different time intervals.

as compared to the product formed, which indicates the formation of some intermediates during the reaction (Fig. 3C). However, there is no significant appearance of a formed intermediate during the reaction in the solution phase, indicating the strong adsorption over the catalyst.

Computational studies, mechanistic study and plausible catalytic cycle

To investigate the hydrazine dehydrogenation mechanism on the V$_2$O$_5$/TiO$_2$ surface and its subsequent catalytic activity in the reduction of nitrobenzene to aniline, we conducted a comprehensive first-principles study utilizing density functional theory (DFT) calculations within the Vienna *ab initio* Simulation Package (VASP). The interactions between core and valence electrons were modeled using projector augmented wave (PAW) potentials. The exchange–correlation energy density functional was treated with the generalized gradient approximation (GGA) of Perdew–Burke–Ernzerhof (PBE), and dispersion interactions were accounted for using Grimme's D3 semi-empirical method (PBE-D3). For the expansion of wavefunctions for the valence electrons, a plane-wave basis set was employed with a kinetic energy cutoff of 520 eV, ensuring accurate representation of electronic behavior. To minimize interactions in the non-periodic direction, a vacuum layer of 20 Å was incorporated. The positions of all atoms were optimized by relaxing them under a constant volume constraint, with a force cutoff set at 0.01 eV Å^{-1} to reach a stable atomic configuration.

The crystal structure of anatase TiO$_2$ was retrieved from the ICSD and subsequently optimized. The measured optimized cell parameters were determined to be $a = b = 3.789$ Å and $c = 9.593$ Å. To investigate the interaction of V$_2$O$_5$ with the TiO$_2$ surface, we focused on the (001) surface of TiO$_2$, whose optimized cell parameters were determined to be 3.703 Å. To create a suitable model for V$_2$O$_5$ adsorption, a $3 \times 3 \times 1$ supercell of the optimized (001) TiO$_2$ surface was constructed and optimized for the adsorption of V$_2$O$_5$ units. The resulting structure of this supercell is depicted in Fig. 4. This approach allowed us to generate the final catalyst model, V$_2$O$_5$/TiO$_2$(001), based on the reconstructed anatase-V$_2$O$_5$ model utilized in previous studies. In the final model, one unit of V$_2$O$_5$ is loaded onto the $3 \times 3 \times 1$ anatase surface, interacting with 45 Ti atoms and 90 O atoms. The optimized structure is presented in Fig. 4(A). Key structural parameters within the V$_2$O$_5$/TiO$_2$(001) model include a V–V distance of 3.281 Å and three distinct V–O distances: bridged O (1.792 Å), terminal O (1.598 Å), and Ti-bound O (1.775 and 1.759 Å).

The dehydrogenation of hydrazine on an optimized catalyst surface was thoroughly investigated, and the results are depicted in Fig. 5. In the most energetically favorable configuration of N$_2$H$_4$ adsorbed on the catalyst surface, the shortest distance between a nitrogen atom (N) and a vanadium atom (V) was found to be 2.305 Å. The hydrogen atoms of N$_2$H$_4$ interacted with the surface through hydrogen bonding, resulting in an adsorption energy of 88.76 kJ mol^{-1}. From this adsorbed N$_2$H$_4$ structure, we examined the transfer of one of the hydrogen atoms from the hydrazine molecule to various oxygen sites bound to both V and Ti atoms. It was observed that the transfer
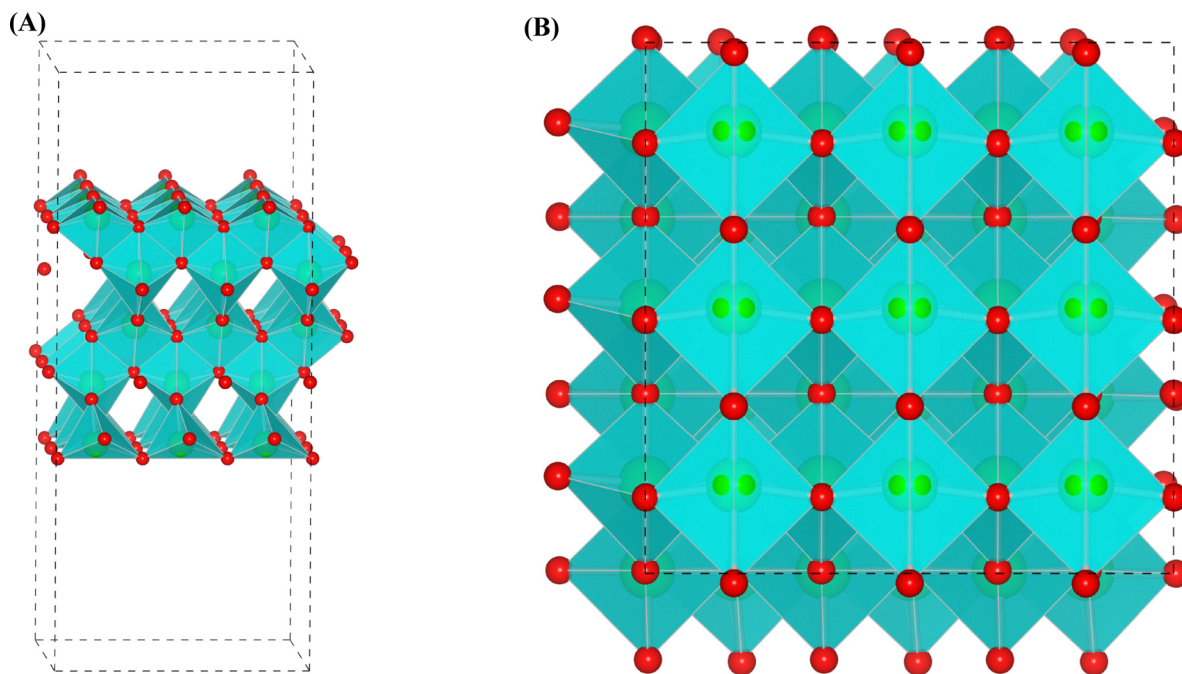
Fig. 4 Optimized structure of the TiO$_2$ (001) surface: (A) side and (B) top views.
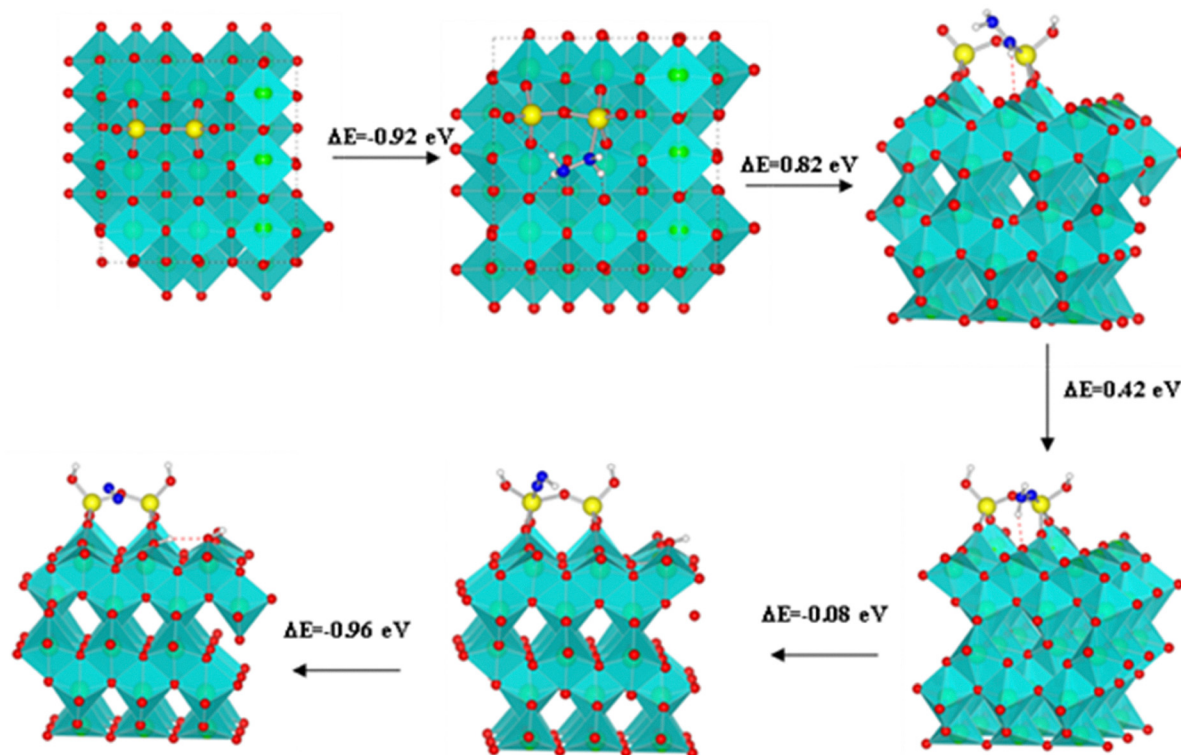

Fig. 5 Schematic representation of dehydrogenation of N$_2$H$_4$ over V$_2$O$_5$/TiO$_2$.

of hydrogen to an oxygen site bound to vanadium (V) was energetically preferred. However, this particular transfer was endothermic, requiring an input energy of 79.12 kJ mol^{-1}. Additionally, the shortest V–N distance in the optimized structure was shortened compared to the initial 2.305 Å, measuring

1.927 Å. For the subsequent hydrogen transfer, we investigated the transfer of a hydrogen atom bound to a nitrogen (N) atom to different oxygen sites. The transfer of a hydrogen atom from an N atom, bound to a single hydrogen (H), to the second oxygen site bound to vanadium (V) was favored. In this case, the

shortest V–N distance was further reduced to 1.707 Å, and this transfer was also found to be endothermic, requiring an input energy of 40.53 kJ mol^{-1}. In the following two consecutive hydrogen transfer steps, hydrogen atoms from the NH$_2$ group were transferred to oxygen sites bound to titanium (Ti) on the surface. These transfers resulted in the physisorption of an N$_2$ molecule on the catalyst surface, as illustrated in Fig. 5. Notably, both of these hydrogen transfer steps were exothermic, releasing energy in the amounts of 7.72 kJ mol^{-1} and 92.62 kJ mol^{-1}, respectively.

The catalytic reduction of nitrobenzene to aniline over a hydrogenated catalyst has been investigated in detail, and the step-by-step intermediate reactions are depicted in Fig. 6. The adsorption energy of the nitrobenzene molecule on the hydrogenated catalyst is calculated to be −94.55 kJ mol^{-1}. In the optimized structure, the shortest distance between the V-nitro oxygen and the catalyst surface is found to be 2.162 Å, while the other V–O(–NO$_2$) distance is 2.613 Å. The first step involves the transfer of a hydrogen atom from the V-bound oxygen to both nitro oxygen atoms. The minimum energy structure corresponds to the transfer of hydrogen to the oxygen farther from the V site, as shown in Fig. 6. This intermediate reaction has an energy change of −4.82 kJ mol^{-1}. For the subsequent hydrogen
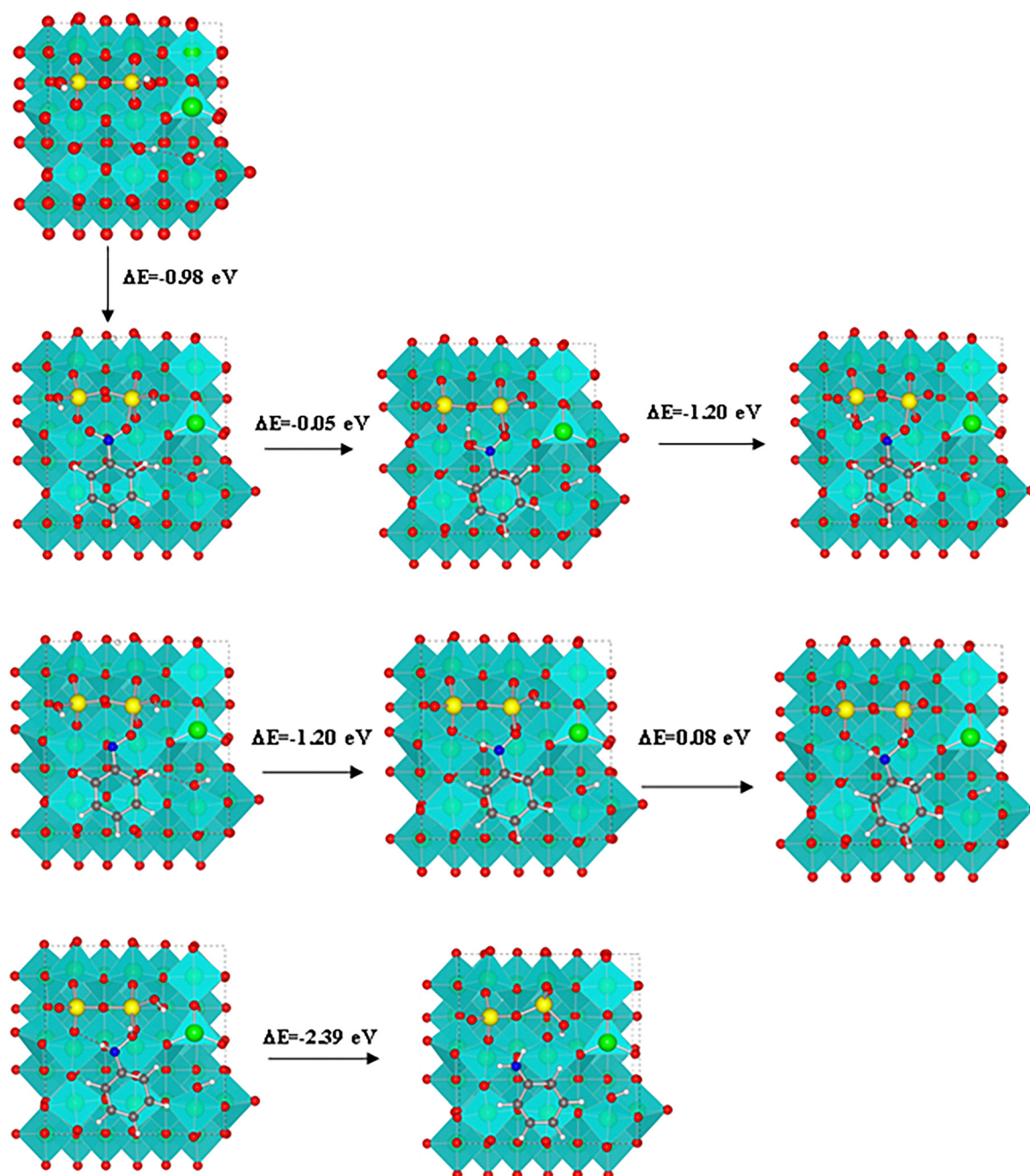

Fig. 6   Schematic representation of catalytic reduction of nitrobenzene to aniline over hydrogenated V$_2$O$_5$/TiO$_2$.
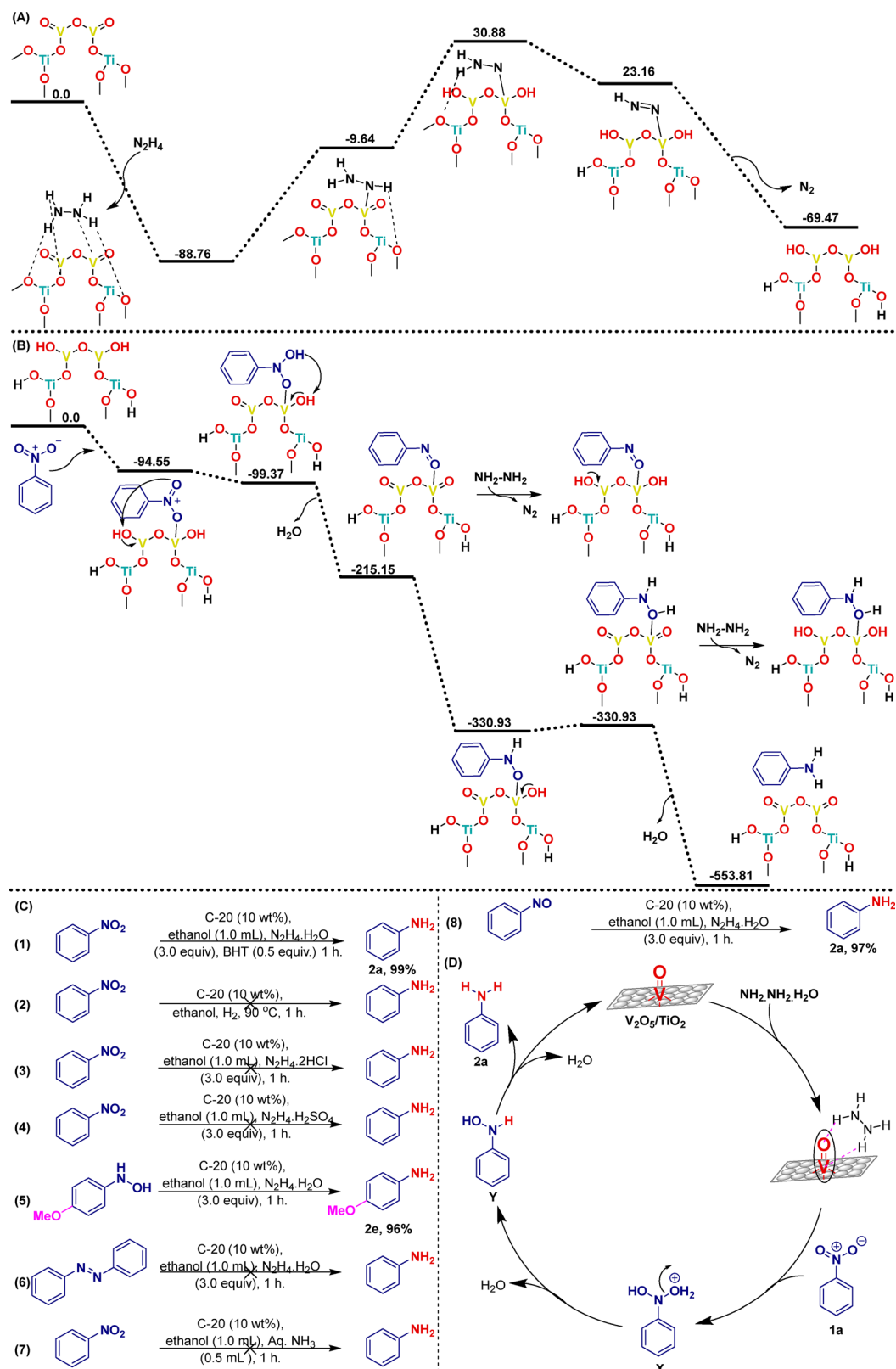
Fig. 7 (A) Reaction energy profile of dehydrogenation of N_2H_4 over the V_2O_5/TiO_2 (001) surface (reaction energies are labelled in kJ mol^{-1}), (B) reaction energy profile of nitrobenzene reduction to aniline over hydrogenated V_2O_5/TiO_2(001) (reaction energies are labelled in kJ mol^{-1}), (C) control experiments and (D) plausible mechanism.

transfer, we considered the transfer of hydrogen from the oxygen bound to the V site to both the –O and –OH of Ph–NOOH. The preferred path involves transferring the hydrogen to the –OH, leading to the separation of a water molecule, with Ph–NO remaining bound to the catalyst surface. In this configuration, the V–O(Ph–NO) distance is found to be 1.979 Å. At this point, we focused on the hydrogenation of the two terminal oxygen atoms bound to the V sites to explore further intermediate reactions in the nitrobenzene reduction. Starting from the Ph–NO bound hydrogenated catalyst surface, we considered the transfer of one hydrogen atom from the V-bound oxygen to both the N and O sites of Ph–NO. This results in the formation of Ph–NHO, with an energy change of -115.78 kJ mol^{-1} and a V–O(Ph–NHO) distance of 1.941 Å in the optimized structure. The subsequent hydrogen transfer from the Ph–NHOH species is slightly endothermic with a reaction energy of 7.72 kJ mol^{-1}. To proceed, one of the V-bound oxygen atoms is hydrogenated, and the transferred OH group binds to the V site. This results in the formation of aniline adsorbed over the catalyst, as shown in Fig. 6. This final reaction is highly exothermic, with a reaction energy of -230.60 kJ mol^{-1}. For a comprehensive overview of the reaction energy profiles, Fig. 7A and B display the profiles for both the dehydrogenation of hydrazine and the reduction of nitrobenzene to aniline, respectively.

To further support the mechanistic insights of the developed protocol, a series of control experiments were conducted. Initial optimization studies were carried out using V$_2$O$_5$ and TiO$_2$ separately, which resulted in no reaction, indicating the lack of their direct involvement in the reaction. Subsequent experiments employing different synthesized catalysts (C-05, C-10, and C-20) revealed an increase in the product yield. This observation highlights the pivotal role of vanadium loading on titanium oxide in enhancing the product yield. An increase in vanadium loading augments the catalyst's acidity, facilitating its interaction with hydrazine hydrate. In a radical scavenger experiment using butylated hydroxytoluene, it was found that the product yield remained unaffected, confirming that the reaction does not proceed through a radical mechanism (Fig. 7C, **1**). Furthermore, the introduction of molecular hydrogen had no impact on product formation, ruling out the involvement of molecular hydrogen in the reaction (Fig. 7C, **2**). The effect of different hydrazine salts on the reaction was also investigated using hydrazine dihydrochloride and hydrazine sulphate instead of hydrazine hydrate, leading to complete cessation of the reaction (Fig. 7C, **3** and **4**). This indicated that the hydrochloride and sulphate salts interfered with the interaction between hydrazine and the catalyst, preventing any reaction. Typically, the reduction of nitroarenes involves the formation of two intermediates: hydroxylamine and azobenzene. However, in this case, mass spectrometry analysis of the reaction mixture did not detect the azobenzene intermediate. To identify the active intermediate generated during the reaction, a reaction with hydroxylamine was performed, yielding an excellent yield of the desired aniline. This result confirmed the generation of the hydroxylamine intermediate during the reaction (Fig. 7C, **5**). In contrast, a reaction with azobenzene did not

yield the respective aniline, indicating that the reaction does not follow the azobenzene formation pathway (Fig. 7C, **6**). The reduction of nitrobenzene did not produce the corresponding aniline when conducted in an aqueous ammonia solution (Fig. 7C, **7**), providing evidence that ammonia is not involved in the reaction. Lastly, nitroso benzene yielded the respective aniline in excellent yield under the developed reaction conditions, confirming the role of the nitroso benzene intermediate in the reaction (Fig. 7C, **8**).

Based on the outcomes and findings from our mechanistic experiments, we have formulated a plausible reaction mechanism for the catalytic reduction of nitroarenes using V$_2$O$_5$/TiO$_2$ as the catalyst. The reaction initiates with the interaction between hydrazine hydrate and nitroarenes in the presence of the catalyst. This interaction leads to the formation of an intermediate species known as the hydroxyl(phenyl)aminooxonium ion, denoted as X. Subsequently, intermediate X undergoes a transformation, eliminating a water molecule in the process, and giving rise to another intermediate, hydroxylamine, labeled as Y. This conversion is crucial in the reaction pathway. Finally, complex Y undergoes further reduction to yield the corresponding amine product, denoted as **2a**. Simultaneously, this step releases the catalytic species necessary for the commencement of the next catalytic cycle (as illustrated in Fig. 7D).

Conclusion

In summary, we have successfully devised an efficient protocol utilizing a heterogeneous V$_2$O$_5$/TiO$_2$ catalyst for the reduction of various (hetero)aromatic and unsaturated nitro compounds to their corresponding amines. This methodology demonstrates remarkable versatility, accommodating a wide range of functional groups and substrates. To illustrate its practicality, we applied this protocol to synthesize seven pivotal pharmaceuticals (paracetamol, methacetin, phenacetin, 4-amino benzoic acid, benzocaine, butamben, and bromhexine), as well as 47 (hetero)arylamine and 12 N-alkylated secondary amines. Our system offers an eco-friendly and efficient approach for generating aniline derivatives, yielding excellent results. Importantly, the only by-products produced are environmentally benign N$_2$ and H$_2$O. Furthermore, we have successfully achieved the one-pot reductive alkylation of nitroarenes using alkyl halides. The catalyst is recyclable, and the protocol can be scaled up for multi-gram synthesis, underscoring its translational potential. Additionally, the protocol demonstrates remarkable chemoselectivity, making it a valuable tool for synthetic applications. To gain a more profound insight into the V$_2$O$_5$/TiO$_2$ catalyst, we implemented a multifaceted strategy that encompassed a synergistic blend of density functional theory (DFT) calculations and precisely controlled experimental investigations.

Author contributions

R. U. contributed to preparing the catalyst, optimization, substrate scope for all tables, mechanistic study, data analysis, and

manuscript writing. S. K. assisted in the analysis of the substrate scope. K. S. contributed to computational studies. K. R. S. C. contributed to computational studies and editing of the manuscript. C. S. G. contributed to XPS analysis and editing of the manuscript. S. K. M. conceived and supervised the experiments, data analysis, editing of the manuscript, and overall guidance.

Conflicts of interest

CSIR-IHBT Palampur has filed a patent on the process reported herein. Inventors: Maurya, Sushil Kumar; Upadhyay, Rahul; and Kumar, Shashi. Applicant: Council of Scientific and Industrial Research. International Publication Number: WO 2023/058050 A1.

Data availability

The data underlying this study are available in the published article and its online SI. Supplementary information: The ^{1}H and ^{13}C NMR spectra for all products (PDF). See DOI: https://doi.org/10.1039/d5ma00711a

Acknowledgements

References

1 J. Song, Z. F. Huang, L. Pan, K. Li, X. Zhang, L. Wang and J. J. Zou, Review on selective hydrogenation of nitroarene by catalytic, photocatalytic and electrocatalytic reactions, *Appl. Catal., B*, 2018, **227**, 386–408.

2 C. Fleischmann, M. Lievenbruck and H. Ritter, Polymers and dyes: developments and applications, *Polymers*, 2015, **7**, 717–746.

3 A. Y. Guan, C. L. Liu, G. Huang, H. C. Li, S. L. Hao, Y. Xu and Z. N. Li, Design, synthesis, and structure−activity relationship of novel aniline derivatives of chlorothalonil, *J. Agric. Food Chem.*, 2013, **61**, 11929–11936.

4 K. Naksomboon, J. Poater, F. M. Bickelhaupt and M. A. F. Ibanez, Para-Selective C−H Olefination of Aniline Derivatives via Pd/S,O ligand catalysis, *J. Am. Chem. Soc.*, 2019, **141**, 6719–6725.

5 D. Formenti, F. Ferretti, F. K. Scharnagl and M. Beller, Reduction of nitro compounds using 3d-non-noble metal catalysts, *Chem. Rev.*, 2019, **119**, 2611–2680.

6 M. Orlandi, D. Brenna, R. Harms, S. Jost and M. Benaglia, Recent developments in the reduction of aromatic and aliphatic nitro compounds to amines, *Org. Process Res. Dev.*, 2018, **22**, 430–445.

7 H. K. Kadam and S. G. Tilve, Advancement in methodologies for reduction of Nitroarenes, *RSC Adv.*, 2015, **5**, 83391–83407.

8 H. Goksua, H. Sertb, B. Kilbas and F. Sen, Recent advances in the reduction of nitro compounds by heterogenous catalysts, *Curr. Org. Chem.*, 2017, **21**, 794–820.

9 G. Yan and M. Yang, Recent advances in the synthesis of aromatic nitro compounds, *Org. Biomol. Chem.*, 2013, **11**, 2554–2566.

10 F. Li, J. Cui, X. Qian and R. Zhang, A novel strategy for the preparation of arylhydroxylamines: chemoselective reduction of aromatic nitro compounds using bakers' yeast, *Chem. Commun.*, 2004, 2338–2339.

11 D. Kuzmich and C. Mulrooney, Synthesis of 2-aryl-1-hydroxyazaindoles and 2-arylazaindoles via oxidation of O-hydroxyaminostyrylpyridines, *Synthesis*, 2003, 1671–1678.

12 E. Merino, Synthesis of azobenzenes: the colored pieces of molecular materials, *Chem. Soc. Rev.*, 2011, **40**, 3835–3853.

13 Y. Teng, X. Wang, M. Wang, Q. Liu, Y. Shao, H. Li, C. Liang, X. Chen and H. Wang, A Schiff base modified Pt nanocatalyst for highly efficient synthesis of aromatic azo compounds, *Catalysts*, 2019, **9**, 339.

14 A. M. Tafesh and J. Weiguny, A review of the selective catalytic reduction of aromatic nitro compounds into aromatic amines, isocyanates, carbamates, and ureas using CO, *Chem. Rev.*, 1996, **96**, 2035–2052.

15 Z. Li, X. Xu, X. Jiang, Y. Li, Z. Yuc and X. Zhang, Facile reduction of aromatic nitro compounds to aromatic amines catalyzed by support-free nanoporous silver, *RSC Adv.*, 2015, **5**, 30062–30066.

16 S. Sun, Z. Quan and X. Wang, Selective reduction of nitro-compounds to primary amines by nickel-catalyzed hydrosilylative reduction, *RSC Adv.*, 2015, **5**, 84574–84577.

17 S. Fountoulaki, V. Daikopoulou, P. L. Gkizis, I. Tamiolakis, G. S. Armatas and I. N. Lykakis, Mechanistic studies of the reduction of nitroarenes by NaBH$_4$ or hydrosilanes catalyzed by supported gold nanoparticles, *ACS Catal.*, 2014, **4**, 3504–3511.

18 P. Tomkins, E. G. Henke, W. Leitner and T. E. Muller, Concurrent hydrogenation of aromatic and nitro groups over carbon-supported ruthenium catalysts, *ACS Catal.*, 2015, **5**, 203–209.

19 X. Chen, X. Y. Zhou, H. Wu, Y. Z. Lei and J. H. Li, Highly efficient reduction of nitro compounds: Recyclable Pd/C-catalyzed transfer hydrogenation with ammonium formate or hydrazine hydrate as hydrogen source, *Synth. Commun.*, 2018, **48**, 2475–2484.

20 R. J. Rahaim and R. E. Maleczka, Pd-Catalyzed silicon hydride reductions of aromatic and aliphatic nitro groups, *Org. Lett.*, 2005, **7**, 5087–5090.

21 T. Satoh, N. Mitsuo, M. Nishiki, Y. Inoue and Y. Ooi, Selective reduction of aromatic nitro compound with

sodium borohydride-stannous chloride, *Chem. Pharm. Bull.*, 1981, **29**, 1443–1445.

22 S. Kumar and S. K. Maurya, Heterogeneous V_2O_5/TiO$_2$-mediated photocatalytic reduction of nitro compounds to the corresponding amines under visible light, *J. Org. Chem.*, 2023, **88**, 8690–8702.

23 L. Zhao, C. Hu, X. Cong, G. Deng, L. L. Liu, M. Luo and X. Zeng, Cyclic (alkyl)(amino) carbene ligand-promoted nitro deoxygenative hydroboration with chromium catalysis: Scope, mechanism, and applications, *J. Am. Chem. Soc.*, 2021, **143**, 1618–1629.

24 R. V. Jagadeesh, A. E. Surkus, H. Junge, M. M. Pohl, J. Radnik, J. Rabeah, H. Huan, V. Schünemann, A. Brückner and M. Beller, Nanoscale Fe_2O_3-based catalysts for selective hydrogenation of nitroarenes to anilines, *Science*, 2013, **342**, 1073–1076.

25 Z. Zhao, H. Yang, Y. Li and X. Guo, Cobalt-modified molybdenum carbide as an efficient catalyst for chemoselective reduction of aromatic nitro compounds, *Green Chem.*, 2014, **16**, 1274–1281.

26 J. Schneekonig, B. Tannert, H. Hornke, M. Beller and K. Junge, Cobalt pincer complexes for catalytic reduction of nitriles to primary amines, *Catal. Sci. Technol.*, 2019, **9**, 1779–1783.

27 M. Boronat, P. Concepción, A. Corma, S. González, F. Illas and P. Serna, A molecular mechanism for the chemoselective hydrogenation of substituted nitroaromatics with nanoparticles of gold on TiO$_2$ catalysts: a cooperative effect between gold and the support, *J. Am. Chem. Soc.*, 2007, **129**, 16230–16237.

28 J. Song, Z. F. Huang, L. Pan, K. Li, X. Zhang, L. Wang and J. J. Zou, Review on selective hydrogenation of nitroarene by catalytic, photocatalytic and electrocatalytic reactions, *Appl. Catal., B*, 2018, **227**, 386–408.

29 R. H. Crabtree, Deactivation in homogeneous transition metal catalysis: causes, avoidance, and cure, *Chem. Rev.*, 2015, **115**, 127–150.

30 D. R. Padron, A. R. P. Santiago, A. M. Balu, M. J. M. Batista and R. Luquea, Environmental catalysis: present and future, *ChemCatChem*, 2019, **11**, 18–38.

31 X. Hu, X. Sun, Q. Song, Y. Zhu, Y. Long and Z. Dong, N, S co-doped hierarchically porous carbon materials for efficient metal-free catalysis, *Green Chem.*, 2020, **22**, 742–752.

32 S. Chen, L. L. Ling, S. F. Jiang and H. Jiang, Selective hydrogenation of nitroarenes under mild conditions by the optimization of active sites in a well-defined Co@NC catalyst, *Green Chem.*, 2020, **22**, 5730–5741.

33 R. Upadhyay, R. Rana, A. Sood, V. Singh, R. Kumar, V. C. Srivastava and S. K. Maurya, Heterogeneous vanadium catalyzed oxidative cleavage of olefins for sustainable synthesis of carboxylic acids, *Chem. Commun.*, 2021, **57**, 5430–5433.

34 D. S. Surry and S. L. Buchwald, Dialkylbiaryl phosphines in Pd-catalyzed amination: a user's guide, *Chem. Sci.*, 2011, **2**, 27–50.

35 S. V. Ley and A. W. Thomas, Modern synthetic methods for copper-mediated C(aryl)-O, C(aryl)-N, and C(aryl)-S bond formation, *Angew. Chem., Int. Ed.*, 2003, **42**, 5400–5449.

36 M. S. Thakur, O. S. Nayal, R. Upadhyay, N. Kumar and S. K. Maurya, 2-Aminoquinazolin-4(3*H*) one as an Organocatalyst for the Synthesis of Tertiary Amines, *Org. Lett.*, 2018, **20**, 1359–1362.

37 O. S. Nayal, M. S. Thakur, M. Kumar, N. Kumar and S. K. Maurya, Ligand-free iron(II)-catalyzed N-alkylation of hindered secondary arylamines with non-activated secondary and primary alcohols via a carbocationic pathway, *Adv. Synth. Catal.*, 2018, **360**, 730–737.

38 J. C. Castillo, J. O. Hernández and J. Portilla, Cs$_2$CO$_3$-Promoted direct N-alkylation: highly chemoselective synthesis of N-alkylated benzylamines and anilines, *Eur. J. Org. Chem.*, 2016, 3824–3835.

39 C. W. Cheung and X. Hu, Amine synthesis via iron-catalyzed reductive coupling of nitroarenes with alkyl halides, *Nat. Commun.*, 2016, **7**, 12494.

40 M. Rauser, C. Ascheberg and M. Niggemann, Electrophilic amination with nitroarenes, *Angew. Chem., Int. Ed.*, 2017, **129**, 11728–11732.

41 M. Rauser, R. Eckert, M. Gerbershagen and M. Niggemann, Catalyst-free reductive coupling of aromatic and aliphatic nitro compounds with organohalides, *Angew. Chem., Int. Ed.*, 2019, **58**, 6713–6717.

42 S. K. Maurya, P. Patil, S. B. Umbarkar, M. K. Gurjar, M. Dongare, S. Rudiger and E. Kemnitz, Vapor phase oxidation of 4-fluorotoluene over vanadia-titania catalyst, *J. Mol. Catal. A: Chem.*, 2005, **234**, 51–57.

43 R. Upadhyay, S. Kumar and S. K. Maurya, V_2O_5@TiO$_2$ catalyzed green and selective oxidation of alcohols, alkylbenzenes and styrenes to carbonyls, *ChemCatChem*, 2021, **13**, 3594–3600.

44 R. Upadhyay, D. Singh and S. K. Maurya, Highly efficient heterogeneous V_2O_5@TiO$_2$ catalyzed the rapid transformation of boronic acids to phenols, *Eur. J. Org. Chem.*, 2021, 3925–3931.

45 F. Lia, B. Fretta and H. Y. Lia, Selective reduction of halogenated nitroarenes with hydrazine hydrate in the presence of Pd/C, *Synlett*, 2014, 1403–1408.

46 P. R. Loaiza, A. Quintero, R. R. Sotres, J. D. Solano and A. L. Rocha, Synthesis and evaluation of 9-anilinothiazolo[5,4-b]quinoline derivatives as potential antitumorals, *Eur. J. Med. Chem.*, 2004, **39**, 5–10.

47 S. Delarue, S. Girault, F. D. Ali, L. Maes, P. Grellier and C. Sergheraert, One-Pot synthesis and antimalarial activity of formamidine derivatives of 4-anilinoquinoline, *Chem. Pharm. Bull.*, 2001, **49**, 933–937.

48 S. Furukawa, Y. Yoshida and T. Komatsu, Chemoselective hydrogenation of nitrostyrene to aminostyrene over Pd- and Rh-based intermetallic compounds, *ACS Catal.*, 2014, **4**, 1441–1450.

49 J. Mao, W. Chen, W. Sun, Z. Chen, J. Pei, D. He, C. Lv, D. Wang and Y. Li, Rational control of the selectivity of a ruthenium catalyst for hydrogenation of 4-nitrostyrene by strain regulation, *Angew. Chem., Int. Ed.*, 2017, **56**, 11971–11975.

50 I. Sorribes, L. Liu and A. Corma, Nanolayered Co−Mo−S catalysts for the chemoselective hydrogenation of nitroarenes, *ACS Catal.*, 2017, **7**, 2698–2708.

51 J. Corpas, M. T. Quiros, P. Mauleon, R. G. Arrayas and J. C. Carretero, Metal- and photocatalysis to gain regiocontrol

and stereodivergence in hydroarylations of unsymmetrical dialkyl alkynes, *ACS Catal.*, 2019, **9**, 10567–10574.

52 Y. Chen, A. Loredo, A. Gordon, J. Tang, C. Yu, J. Ordoneza and H. Xiao, A noncanonical amino acid-based relay system for site-specific protein labelling, *Chem. Commun.*, 2018, **54**, 7187–7190.

53 J. Yin, J. Zhang, C. Cai, G. J. Deng and H. Gong, Catalyst-free transamidation of aromatic amines with formamide derivatives and tertiary amides with aliphatic amines, *Org. Lett.*, 2019, **21**, 387–392.

54 J. Fischer and C. R. Ganellin, *Analogue-based Drug Discovery*, John Wiley & Sons, 2006, p. 544. ISBN 9783527607495.

55 M. L. Kantam, R. S. Reddy, K. Srinivas, R. Chakravarti, B. Sreedhar, F. Figueras and C. V. Reddy, Platinum nanoparticles supported on zirconia mediated synthesis of N-acyl and N-(tert-butoxycarbonyl)amines from nitroarenes and azides, *J. Mol. Catal. A: Chem.*, 2012, **355**, 96–101.

56 M. Li, L. Hu, X. Cao, H. Hong, J. Lu and H. Gu, Direct Hydrogenation of Nitroaromatics and One-Pot Amidation with Carboxylic Acids over Platinum Nanowires, *Chem. – Eur. J.*, 2011, **17**, 2763–2768.

57 E. M. Nahmed and G. Jenner, Synthesis of anilides by reductive N-acylation of nitroarenes mediated by methyl formate, *Tetrahedron Lett.*, 1991, **32**, 4917–4920.